Utilization of palm fiber as papermaking materials: Microscopic structure and chemical pulping

ZHULIN LI, SHUAI GAO, LEI TANG, DING LIU, QUN LI, GUOYO TIAN, AND ZHAOJIANG WANG

ABSTRACT: The microscopic structure and pulping properties of palm fiber were explored. Soda cooking and sulfate cooking were conducted and compared in terms of physical strength of the obtained pulps. Sulfate pulp showed better performance than soda pulp, as indicated by the 23% higher tensile index, 49% higher tear index, and 36% higher burst index.

To further elevate physical strength, long fibered pulp (LFP), namely commercial softwood sulfate pulp, was mixed with sulfate pulp of palm fiber at levels from 20% to 50%. At the blend level of 50%, tensile index of 52.13 N•m/g, tear index of 15.63 mN•m²/g, and burst index of 3.42 kPa•m²/g were attained. The lignin in spent liquor from pulping was isolated and characterized. Soda lignin of palm fiber was mainly composed of guaiacyl and syringyl units, and showed weight-average molecular weight of 3616 g/mol.

Application: We explored the properties of soda pulp and sulfate pulp of palm fiber. Comparison was made with hardwood and softwood pulp in terms of fiber length and physical strength. The reported results suggested the feasibility of palm fiber for papermaking.

The palm tree is one of the common tree species in tropical areas and has important economic value. Palm trees are not only ornamental plants, but they are also an important source of wood. The leaf of the palm can be used to make palm-bark rain capes. Palm fiber is used to make household goods. As a high-quality natural fiber, palm fiber is not actually fully exploited. Global fiber production has been 107 million metric tons since 2018 and is expected to grow to 145 million metric tons by 2030. No more than 10% of natural plant fibers such as palm and hemp are used [1]. As a type of natural fiber with excellent properties, palm fiber is not only widely planted, but also an abundant source. However, most palm fiber is burned and represents a waste of fiber resources.

The efficient utilization of biomass resources has been realized with the improvement in the population's environmental awareness. In order to realize efficient utilization of palm fiber, biomass refining [2] was introduced. The surface of palm fiber is sags and crests, and the cross section is honeycomb [3], and it has a low degree of crystallinity, a large specific surface area, and large pore cover [4]. The structure and nature of palm fiber determine its application. Upon further study, palm fiber has been widely used; for example, it can be used for bio-composites, and there have been comprehensive reviews on the bio-composites of palm fibers [5]. Polymer matrix composites were prepared by using palm fiber and S-glass [6]. The test results show that the composite material had good adhesion and was a high strength element for structural applications. With epoxy resin as matrix, palm sheath fiber and bagasse fiber were used to prepare composite materials. The experimental results showed that the composite materials had good flexural properties and hardness, and could be used to develop automobile dashboards [7]. The oil palm empty fruit bunch cellulose was dissolved in a sodium hydroxide (NaOH)/urea solvent and mixed with sodium carboxymethylcellulose (NaCMC) and crosslinker epichlorohydrin (ECH) to make a superabsorbent hydrogel [8]. The results showed that the formed hydrogel attained highest gel fraction, water absorption, degree of swelling, and transparency values at 10% of ECH.

Palm fiber has low density and porous structure. Palm fiber was used to prepare activated carbon with good adsorption performance and had a broad application prospect in the field of sewage treatment and air purification [9]. In addition, palm fiber is sustainable and biodegradable, which can change clay properties and provide reference and application for related engineering [10]. Furthermore, oil, natural gas, and other fossil energy reserves have been gradually depleted, and fuel ethanol, a renewable clean energy, has gradually become an important part of the energy structure [11]. Palm fiber has been converted into bioethanol by enzymatic hydrolysis or fermentation [12]. Palm fiber is also a kind of papermaking material with high yield and good properties. The utilization of palm fiber as a papermaking material can not only solve the pollution prob-

lem from fiber waste, it can also alleviate the shortage of raw materials for papermaking [13]. Pulping and biomass refining are new strategies for efficient utilization of palm fiber [14]. Pretreatment of palm fiber removed most of the lignin and increased glucose yield [15]. Many studies have demonstrated the feasibility of palm fiber for pulping and papermaking [16,17].

Early studies focused on chemical pulping of palm fiber by soda and sulfate processes [18-20]. In the present work, in order to explore the pulping property, the microscopic structure of palm fiber was studied by computerized tomography. Chemical pulping was conducted. Also, long fibered pulp (LFP), namely softwood sulfate pulp, was blended with the pulp of palm fiber to improve the physical strength of the paper sheet. The structure of lignin in spent liquor was also characterized.

MATERIALS AND METOHDS

Raw materials and chemicals

Palm fiber was collected from a farm located in Malaysia. The palm fiber was dedusted with hot water before cooking. After air-drying, the fiber was size-reduced to 3–5 cm in length. Sodium hydroxide, sodium sulfide, and anthraquinone were purchased from Sigma Aldrich (St. Louis, MO, USA). All the chemicals were analytical grade in purity and used without further purification.

Chemical pulping and making of handsheets

Laboratory scale pulping experiments were performed in a 15 L vertical rotary autoclave (Kumagai Riki Co. Ltd.; Tokyo) with four bombs of 1 L capacity each. The pulping conditions are listed in **Table I**. The cooking temperature, anthraquinone dosage, liquid-to-solid ratio, and holding time in each case were fixed at 160°C, 0.05%, 1:5(m/v), and 2 h, respectively. The level of sodium hydroxide for the soda process and the sulfate process was same, from 16% to 25% on the mass basis of palm fiber. Sulfidity of the sulfate process was 20%. The spent liquor was separated from the undispersed fiber through filtration and water washing. The undispersed fiber was then mechanically milled using a high-consistency refiner (BR30-300C; Kumagai Riki Kogyo Co. Ltd.) at a disc gap of 0.15 mm or 0.3 mm. The pulp from the soda process and the sulfate process was observed by optical microscope (Axio Scope A1, Zeiss; Oberkochen, Germany). The obtained pulp from the refiner was then beaten to Canadian Standard Freeness from 300±50 mL prior to papermaking. In order to improve the physical strength of paper, LFP was mixed with palm fiber pulp at levels from 20% to 50% for papermaking. The paper sheets of basis weight of 60 g/m² were fabricated by an RK3AKWT sheet former (Frank-PTI GMBH; Birkenau, Germany) according to TAPPI T 205 sp-12 "Forming handsheets for physical tests of pulp."

Samples	Alkali Charge, %	
	Sodium Hydroxide	Sulfidity
Soda-16	16	-
Soda-20	20	-
Soda-25	25	-
Sufate-16	16	20
Sulfate-20	20	20
Sulfate-25	25	20

I. Palm fiber pulping conditions for the soda process and the sulfate process.

Microstructure detection of palm fiber

Micro computerized tomography (micro-CT) was used to obtain cross-sectional images of untreated palm fiber at a resolution of 300 nm. Scanning electron microscope (SEM) was used to obtain surface topography images of palm fiber with a Hitachi Regulus 8220 SEM (Hitachi; Tokyo, Japan) that operated at an acceleration voltage of 5 kV.

Molecular weight determination of lignin

The purified lignin was obtained from spent liquor. First, the liquors were acidified with 72wt% sulfuric acid (H_2SO_4) until reaching pH 2. The resulting precipitates were centrifuged and washed by 0.01M H_2SO_4 or distilled water. Finally, the precipitates were cryo-dried after dialysis. For lignin acetylation, 10 mg purified lignin was transferred into a 5 mL vial. Then, 2.5 mL pyridine and 2.5 mL acetic anhydride solution were added and mixed with lignin. After 72 h at dark, the acetylated lignin sample was obtained after freeze drying. Next, 6 mg acetylated lignin was dissolved in 3 mL tetrahydrofuran (THF) for molecular weight determination by gel permeation chromatography (Waters e2695, NYSE:WAT technology, Waters Corp; Milford, MA, USA). The injection volume was 25 µL. The flow rate was 1 mL/min, and the column (300 mm length × 8 mm diameter, 15 mL volume) temperature was 40°C.

Structure characterization of lignin

Nuclear magnetic resonance (NMR) analysis of lignin, including two-dimensional-heteronuclear single-quantum correlation (2D-HSQC) and proton nuclear magnetic resonance (^{1}H NMR), were conducted using an NMR spectrometer (AVANCE III 400 MHz, Bruker; Billerica, MA, USA) as previously described. About 60 mg lignin was dissolved in 0.5 mL dimethyl sulfoxide-d_6 (DMSO-d_6) solution and transferred to a 5 mL nuclear test cube for testing. Tetramethylsilane (TMS) was used for internal referencing of chemical shifts. The relaxation delay (D1) was 1 s, and the acquisition time was 4.5 s.

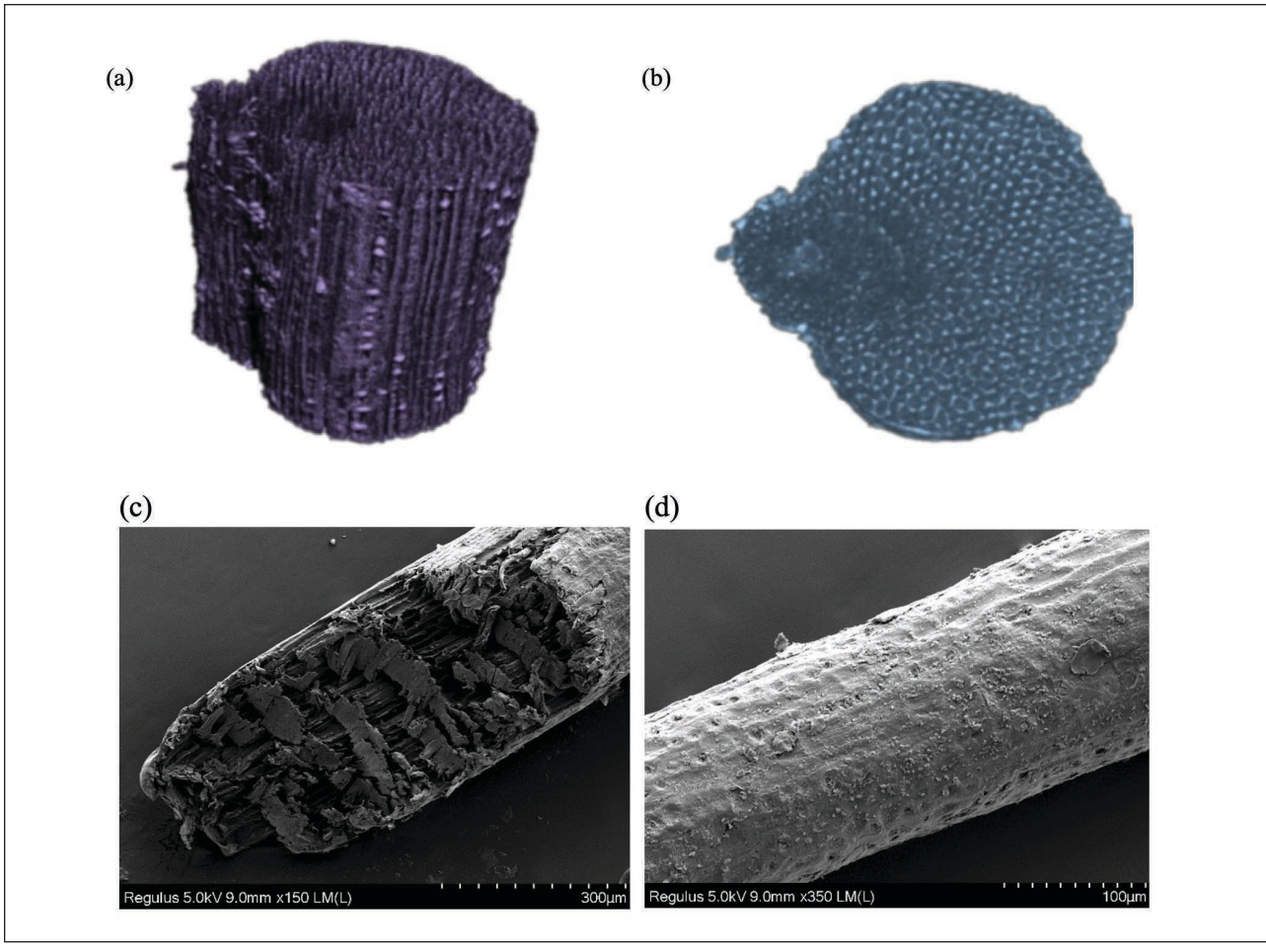

1. The cross-sectional images (a,b) and surface topography images (c,d) of palm fiber obtained by micro computerized tomography (micro-CT) and scanning electron microscope (SEM), respectively.

Determination of physical properties of handsheets

The paper handsheets were prepared using soda and sulfate pulp. For the paper sheets, physical properties were determined, including yield, tensile strength (Chinese National Standard GB/T 12914-2018 "Paper and board – determination of tensile properties – constant rate of elongation method 20 mm/min)," tear strength (GB/T 455-2002 "Paper and board – Determination of tearing resistance"), and burst strength (GB/T 454-2020 "Paper – Determination of bursting strength). All measurements were performed at least three times.

RESULTS AND DISCUSSION

Microscopic structure of palm fiber

The cross-sectional images of untreated palm fiber (**Fig. 1a** and Fig. 1b) were obtained by micro-CT. The surface topography images of palm fiber (Fig. 1c and Fig. 1d) were obtained by SEM. The palm fibers are cylindrical in form with a diameter of about 1.0 mm. Palm fiber is covered with a dense and rough surface. From the cross-sectional image (Fig. 1a), the microfibers are very neatly arranged inside of palm fiber. From the transverse image (Fig. 1b), the xylem cell can be recognized by the gray-colored microfibers and cell corners that are white in color. Zhang et al. [21] also studied the structure and properties of palm leaf sheath fiber. It was reported that the white particles can improve the frictional force and facilitate defibering during the beating process. Christina et al. [22] indicated that the particles were rich in silicon and have a good antibacterial property because of the compact structure of particles.

Yield and physical strength of palm fiber pulp

The pulp yield from the soda process and sulfate process in **Table II** demonstrated that Soda-16 showed the highest pulp yield at 83.4%, which means a mild delignification. Soda-16 actually belonged to chemical mechanical pulp. The micrograph of Soda-16 in **Fig. 2** showed the length of fibers from 0.2–0.4 mm and the width of fibers from 20–30 µm. These dimensional values suggested that the chemical mechanical pulp of palm fiber was very small fines. The yields of Soda-25, Sulfate-16, Sulfate-20, and Sulfate-25 were 45.6%, 49.5%, 45.2%, and 41.8%, respectively, which are

Handsheet Samples	Yield, %	Tensile Index, N•m/g	Tear Index, mN•m²/g	Burst Index, kPa•m²/g	Brightness, %ISO
Soda-16	83.4	22.30	6.48	2.10	19.2
Soda-20	56.3	23.64	6.21	2.03	19.1
Soda-25	45.6	24.90	6.16	1.90	19.1
Sulfate-16	49.5	17.74	4.85	1.89	19.5
Sulfate-20	45.2	25.12	7.09	2.31	19.6
Sulfate-25	41.8	30.61	9.16	2.59	19.2
Sul/LFP-20*	-	28.81	9.82	2.16	22.2
Sul/LFP-40	-	44.91	13.27	2.98	22.8
Sul/LFP-50	-	52.13	15.63	3.42	23.5
LFP		75.80	14.30	5.02	32.3

Sul = Sulfate-16; LFP = long fiber pulp, namely, commercial softwood sulfate pulp; 20 = blend level of 20% LFP, which also follows for 40% and 50% below.

II. Pulp yields from palm fiber for the soda process and the sulfite process, as well as the physical strength of the pulps.

typical values for pulp yield of chemical pulp. The big drop in pulp yield from 83.4% for Soda-16 to 49.5% for Sulfate-16 indicated the positive effects of sulfidity in boosting delignification. The average length of Sulfate-16 fiber was 1.3 mm, which is twice as long as that of Soda-16. Furthermore, the fiber surface of Sulfate-16 became much smoother than Soda-16. From Fig. 2, no significant difference was observed among the microstructures of Sulfate-16, Sulfate-20, and Sulfate-25. It is necessary to make a comparison of fiber length and width between palm fiber pulp and wood pulp. For wood pulp fibers, biometry showed a range in length (0.70–0.84 mm for hardwood, 1.57–1.96 mm for softwood) and in width (18.0–19.1 µm for hardwood, 29.8–37.2 µm for softwood) [23]. For the chemical pulp of palm fiber in Fig. 2, pulp fiber showed an average length of 0.5 mm and an average width of 22 µm. Comparatively, the fiber length of palm fiber pulp was much shorter than wood pulp.

The physical strength of pulps is listed in **Table II**. The tensile index and tear index showed close values for soda pulps, from 22.3 to 24.9 N•m/g. The increase in chemical dosage showed little effect on the tensile strength for soda pulping. On the contrary, the tensile index and tear index depended on chemical dosage for the sulfate pulps. The tensile index increased from 17.74 N•m/g for Sulfate-16 to 30.61 N•m/g for Sulfate-25. The burst index increased from 4.85 mN•m²/g for Sulfate-16 to 9.16 mN•m²/g for Sulfate-25.

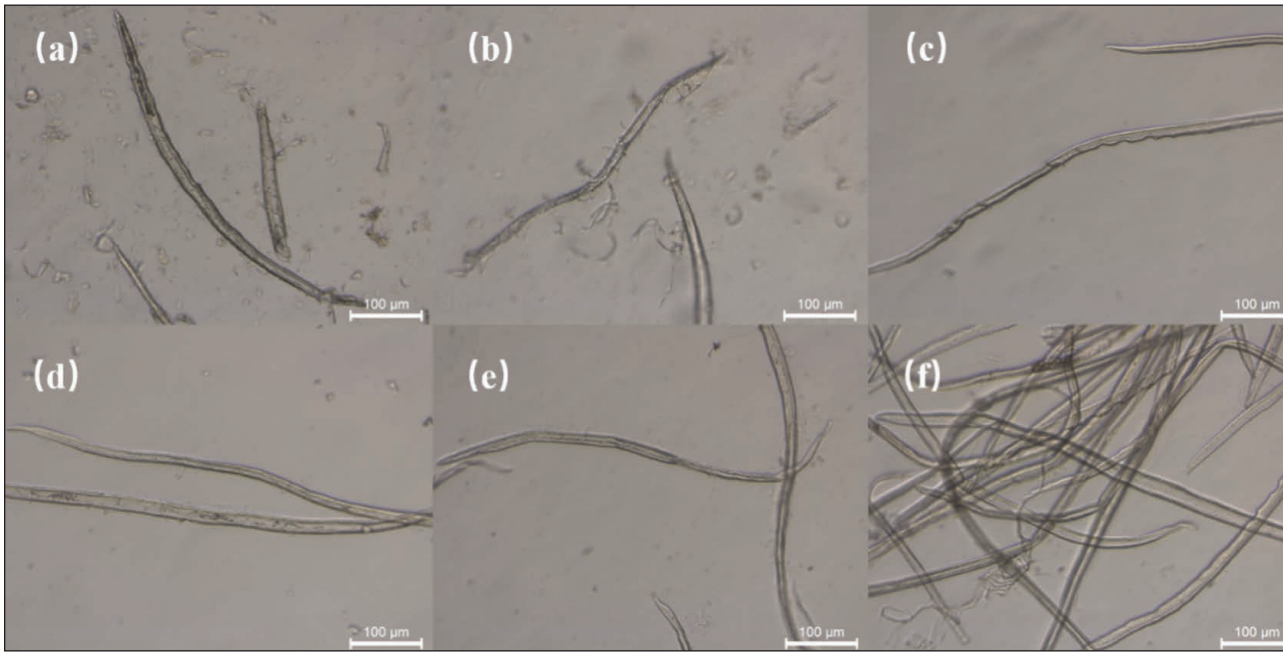

2. Microscope images of pulps from the soda process and the sulfate process: (a) Soda-16, (b) Soda-25, (c)(f) Sulfate-16, (d) Sulfate-20, and (e) Sulfate-25.

Label*	Mw, g/mol	Mn, g/mol	PDI, Mw/Mn	Reference
Soda-palm	3616	1915	1.9	
Indulin kraft	4290	530	8.1	[27]
Soda-P1000	3270	620	5.2	[27]
Alcell	2580	600	4.3	[27]
OS-W	1960	450	4.4	[27]
OS-P	2180	570	3.8	[27]
OS-S	2030	420	4.9	[27]
MAL-Pine	5300	2400	2.2	[28]
MAL-Eucalyptus	5420	2600	2.1	[28]
MAL-Corn stalk	7680	3070	2.5	[28]
MAL-Bamboo	8520	3410	2.5	[28]

* Soda-palm was isolated from spent liquor of Soda-25. Indulin kraft is softwood kraft lignin from Ingevity, North Charleston, SC, USA. Soda-P1000 is soda lignin from mixed wheat straw and Sarkanda grass. Alcell is organosolv lignin from mixed hardwoods of maple, birch, and poplar from Repap Technologies, Vancouver, BC, Canada. OS-W, OS-P, and OS-S are three organosolv lignins extracted from wheat straw, poplar, and spruce, respectively, using the acid-catalyzed ethanol-based organosolv process. MAL-Pine, MAL-Eucalyptus, MAL-Corn stalk, and MAL-Bamboo were obtained by mild acidic dioxane isolation process.

III. Comparison of weight-average molecular weight (Mw), number-average molecular weight (Mn), and polydispersity (PDI) of palm fiber soda lignin with other technical lignins.

Results in Table II also showed that pulp from the sulfate process was superior in physical strength to that from the soda process in physical strength. However, the physical strength of palm fiber pulp was not as good as pulps from other biomass. Wenchao Jia et al. [24] produced kraft pulp from acacia wood with tensile index of 57.63 N•m/g and tear index of 16.93 mN•m²/g. Yuan et al. [25] prepared kraft pulp from bamboo with tensile index of 50.0 N•m/g. Lísias Pereira Novo et al. [26] prepared soda pulp from sugarcane with tensile index of 52.1 N•m/g and burst index of 3.71 kPa•m²/g. In order to improve the physical strength of pulp, LFP was mixed with Sulfate-16 pulp at levels from 20% to 50% for papermaking. The results indicated that the physical properties of the papers were greatly improved. The tear index increased by 102% from 4.85 mN•m²/g for Sulfate-16 to 9.82 mN•m²/g for Sul/LFP-20 with a blend level of 20%. The burst index increased by 57% from 1.89 kPa•m²/g for Sulfate-16 to 2.98 kPa•m²/g for Sul/LFP-40 with a blend level of 40%. In this way, the application of palm fiber in the paper industry is feasible for producing paper products with promising strength.

Molecular weight distribution of soda lignin from palm fiber

The lignin of in spent liquor of Soda-25 was purified and acetylized for molecular weight determination. A wide molecular weight distribution was observed for Soda-25 lignin, ranging from $10^{2.8}$ g/mol to $10^{4.2}$ g/mol (**Fig. 3**). The weight-average molecular weight (Mw), the number-average molecular weights (Mn), and polydispersity (PDI) were 3616 g/mol, 1915 g/mol, and 1.88, respectively. For a better understanding of palm fiber lignin, molecular weight of technical lignins [27] and mild acidolysis lignins [28] (MAL) from softwood, hardwood, and herbaceous biomass are provided in **Table III** for comparison. The Mw of Soda-palm was 3616 g/mol, which is higher than Mw of 3270 g/mol for soda lignin from wheat straw and Sarkanda grass (Soda-P1000), but lower than the Mw of 4290 g/mol for softwood kraft lignin (Indulin kraft, In gevity; North Charleston, SC, USA). It is worth mentioning that the PDI of Soda-palm was closer to

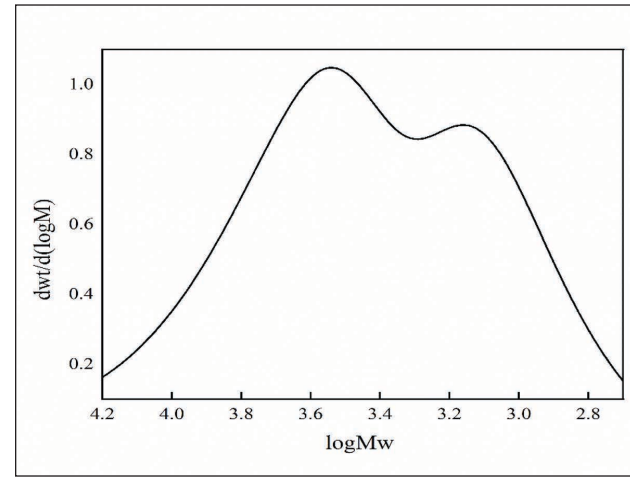

3. Molecular mass distribution of Soda-25 lignin from palm fiber.

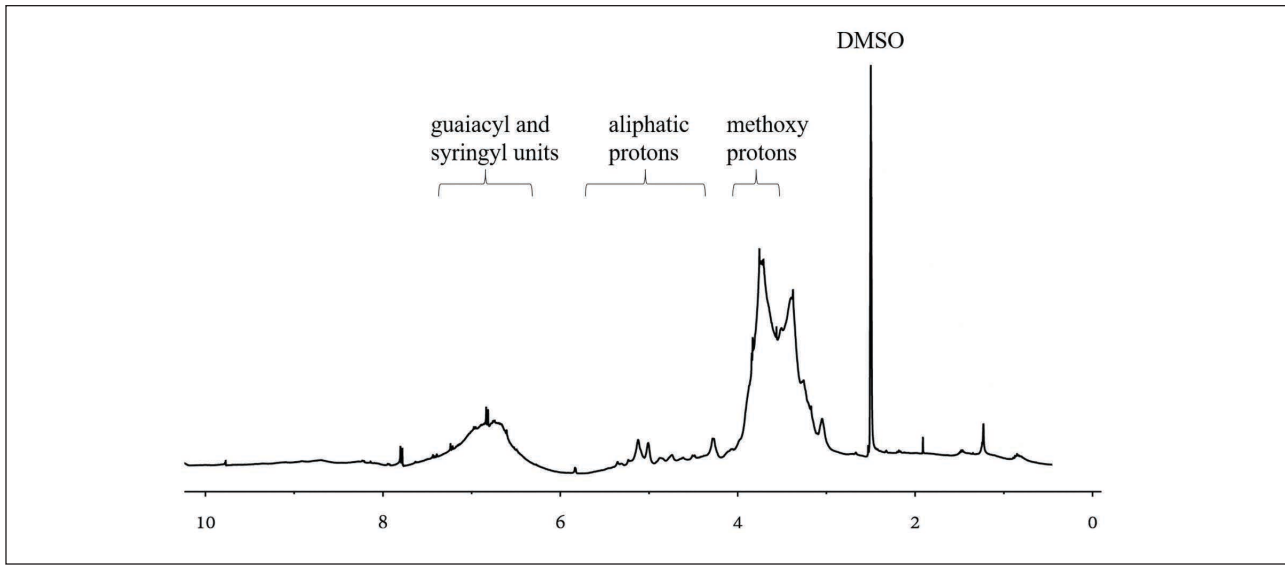

4. Proton nuclear magnetic resonance (1H NMR) spectrum of Soda-25 lignin from palm fiber.

1.0 than any other of the lignins listed in Table III, which indicated better homogeneity or uniformity of lignin molecules. Molecular weight of organosolv lignins (Alcell [Repap Technologies; Vancouver, BC, Canada], OS-W, OS-P, OS-S) were lower than soda and kraft lignin (Soda-palm, Indulin kraft, Soda-P1000). This is possibly attributed to the intense cleavage of lignins during organosolv pulping. Mild acisolysis lignins in Table III were obtained by mild acid dioxane isolation process, and therefore had much higher molecular weight. This was confirmed by comparison of Mw between MAL-Pine and Indulin kraft.

Structural characteristics of lignin

Lignin is a three-dimensional biopolymer built from phenylpropane units, including the guaiacol (G), syringe (S), and *p*-hydroxyphenyl (H) units. The ^{1}H NMR spectrum of palm fiber Soda-25 lignin is shown in **Fig. 4**. According to literature [29], the signal at 6.2–7.5 ppm originates from the aromatic proton. This is mainly the signal of the S unit at 6.2–6.8 ppm and G unit at 6.8–7.3 ppm. The signal of the H unit from 7.3 ppm to 7.5 ppm was comparatively weak, which indicated the low level of H unit in palm fiber Soda-25 lignin. The chemical shift of primarily aliphatic protons

Label	C/H, ppm	Assignment
Methoxyl	53.5/3.04	C_{β}-H_{β} in β-β′resinol substructure (B)
A_{γ}	59.3/3.42 and 3.68	C_{γ}-H_{γ} in γ-hydroxylated β-O-4 substructure (A)
C_{γ}	71.1/3.82 and 4.15	C_{γ}-H_{γ} in β-β′ resinol substructure (C)
C_{α}	87.5/4.5	C_{α}-H_{α} in β-5 resinol substructure (C)
A_{α}(S)	71.7/4.86	C_{α}-H_{α} in β-O-4′substructure(A) linked to an S-unit
A_{β}(G)	83.1/4.28	C_{β}-H_{β} in β-O-4′substructure(A) linked to a G-unit
B_{γ}	65.2/3.64	C_{γ}-H_{γ} in β-5′phenylcoumaran substructures (B)
$S_{2,6}$	103.9/6.69	$C_{2,6}$-$H_{2.6}$ in etherified syringyl unit (S)
$S'_{2.6}$	106.2/7.24	$C_{2,6}$-$H_{2.6}$ in oxidized syringyl unit (S)
G_2	110.9/6.98	C_2-H_2 in guaiacyl unit (G)
G_5	114.9/6.73 and 6.93	C_5-H_5 in guaiacyl unit (G)
$H_{2,6}$	127.8/7.23	$C_{2,6}$-$H_{2,6}$ in the *p*-hydroxycinnamic unit (H)

IV. The ^{13}C-^{1}H NMR spectroscopy corresponding to the main lignin structural units in the heteronuclear single quantum coherence (2D-HSQC) map.

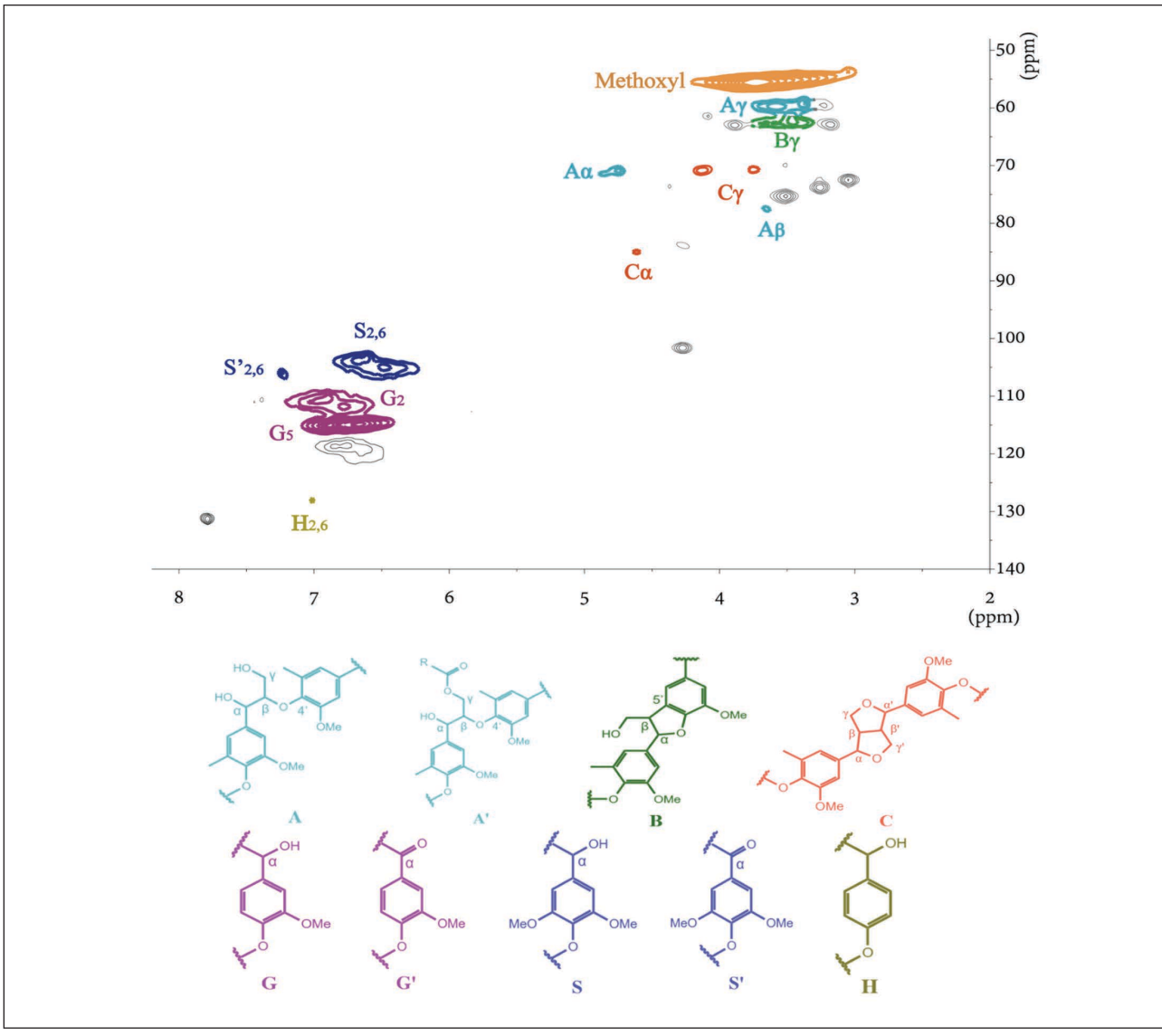

5. The two-dimensional-heteronuclear single-quantum correlation (2D-HSQC) spectra of palm fiber soda lignin: (A) β-O-4′ alkyl-aryl ether; (A′) γ-OH with p-coumaroylated β-O-4′ alkyl-aryl ether; (B) β-5′ phenylcoumaran; (C) β-β′ resinol; (H) p-hydroxyphenyl units; (G) guaiacyl units; and (S) syringyl units.

was located from 4.0 ppm to 6.0 ppm. The proton at 4.3 ppm was attributed to lignin having β-O-4 inter-unit linkages. The strong signal between 3.5 ppm to 4.0 ppm was attributed to protons in methoxy (-OCH_3) of lignin.

To obtain more detailed chemical information on the lignin, quantitative 2D-HSQC NMR of the Soda-25 lignin from palm fiber was conducted. The heteronuclear single quantum coherence (2D-HSQC) spectrum of palm fiber Soda-25 lignin is shown in **Fig. 5**. The structures were assigned to NMR signals [30], according to **Table IV**. In Fig. 5, β-O-4 (A), β-5 (B), and β-β (C) interunit linkages were identified in the palm fiber Soda-25 lignin. Compared with the β-O-4 (A) substructures, notably, phenylcoumaran β-5 (B) was at a higher level. In the aromatic region, the signals of guaiacyl (G) and syringyl (S) units were strong, while the signal of the p-hydroxyphenyl (H) unit was quite weak. The proportion of S:G:H was 1:1:0.09. This indicated that very few p-hydroxyphenyl (H) units were present in palm fiber Soda-25 lignin, which is consistent with the results of ^{1}H NMR analysis.

CONCLUSION

The microscopic structure of palm fiber was studied by micro-CT and SEM. The pulp was obtained by the soda process and the sulfate process. Microscopic analysis demonstrated that the palm pulp fibers were shorter than woody fibers. The physical strength of pulp was greatly improved by adding LPF. Soda lignin from palm fiber had higher molecular weight than hardwood. Structural characterization by NMR revealed the lignin was composed of G and S units. **TJ**

ACKNOWLEDGEMENT

The authors kindly acknowledge funding support (ZR2021MB129) from the Department of Science and Technology of Shandong Province.

LITERATURE CITED

1. Chares, S.M. and Perumalsamy, M., J. *Cleaner Prod.* 05: 100304(2021).
2. Kumar, A.M., Surendra, S., Anil, P., et al., *Renewable Sustainable Energy Rev.* 127(C): 109876(2020).
3. Chen, C.J., Zhang, Y., Wang, G.H., *J. Donghua Univ.* 31(5): 617(2014).
4. Zhang, T.H., Guo, M., Cheng, L., et al., *Cellulose* 22(2): 1039(2015). https://doi.org/10.1007/s10570-015-0570-x.
5. Senthilkumar, K., Saba, N., Rajini, N., et al., *Constr. Build. Mater.* 174(20): 713(2018). https://doi.org/10.1016/j.conbuildmat.2018.04.143.
6. Venkatesan, S.P., Boobalan, L., Bennet, S., et al., *Mater. Today: Proc.* 47(P14): 4373(2021). https://doi.org/10.1016/j.matpr.2021.05.184.
7. Marichelvam, M.K., Manimaran, P., Verma, A., et al., *Polym. Compos.* 42(1): 512(2021). https://doi.org/10.1002/pc.25843.
8. Salleh, K.M., Zakaria, S., Sajab, M.S., et al., *Int. J. Biol. Macromol.* 118(Pt.B): 1422(2018). https://doi.org/10.1016/j.ijbiomac.2018.06.159.
9. Ooi, C.H., Cheah, W.K., Sim, Y.L., et al., *J. Environ. Manage.* 197(15): 199(2017). https://doi.org/10.1016/j.jenvman.2017.03.083.
10. Qu, J. and Zhu, H., *J. Renewable Mater.* 9(4): 767(2021). https://doi.org/10.32604/jrm.2021.013816.
11. Tuandung, H. and Nhuan, N., *Fermentation* 7(4): 314(2021).
12. Ragab Tamer, I.M., Alminderej Fahad, M., ElSayed Wael, A., et al., *Sustainability* 13(24): 13660(2021). https://doi.org/10.3390/su132413660.
13. Saferi, S.K.A. and Yusof, Y., *Appl. Mech. Mater.* 315: 443(2012). https://doi.org/10.4028/www.scientific.net/AMM.315.443.
14. Gomes, F.J.B., Santos, F.A., Colodette, J.L., et al., *Nat. Resour.* 5(9): 419(2014). https://doi.org/10.4236/nr.2014.59039.
15. Palamae, S., Dechatiwongse, P., Choorit, W., et al., *Carbohydr. Polym.* 155(2): 491(2017). https://doi.org/10.1016/j.carbpol.2016.09.004.

ABOUT THE AUTHORS

Palm fiber is abundant in South Africa, and many companies would like to use it as a pulping material. The fiber is very hard and dense in structure, and it is very difficult to dissolve the lignin and isolate the cellulose fibers. For this reason, the microscopic structure of palm fiber was first observed by micro-CT. Most importantly, microscopic images of the pulp fibers were obtained. Comparison was made with other woody fibers. This was very helpful in the explanation of pulp strength.

The cellulose fibers from palm are short compared with woody fibers. The most difficult aspect of this research was determining how to make the paper handsheet strong enough. To address this, we blended in long-fibered softwood kraft pulp at various levels, which was very helpful.

We found that cellulose pulp contains mainly short fibers and fines, which explains the low physical strength of pulp. It was very interesting to see that microfibers in palm fiber are very neatly arranged in the vertical direction.

This study informs mills of the pulping conditions for palm fiber. In addition, it provides a good understanding of this pulp fiber's biometry, including width and length, as well as its difference from woody pulp fibers.

As physical strength is very important, a new pulping process should be developed for palm fiber that can isolate its long fibers and keep the integrity of the fibers.

Li, Z.

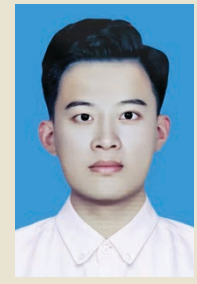

Gao

Tang

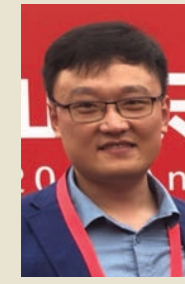

Liu

Li, Q.

Tian

Wang

Z. Li and Gao are master's degree candidates, Tian is assistant professor, and Wang is professor at the State Key Laboratory of Biobased Material and Green Papermaking, Qilu University of Technology (Shandong Academy of Sciences), in Jinan, China. Tang is technical director and Liu is manager of the Technical Department at Shengquan Group Co. Ltd., in Jinan, China. Q. Li is professor at Tianjin University of Science and Technology in Tianjin, China. Email Wang at wzj@qlu.edu.cn.

16. Daud, W.R.W. and Law, K.N., *BioResources* 6(1): 901(2011). https://doi.org/10.15376/biores.6.1.901-917.
17. Jarupan, L., Hunsa Udom, R., and Bumbudsanpharoke, N., *J. Nat. Fibers* 19(7): 2772(2021). https://doi.org/10.1080/15440478.2021.1889433.
18. Jiménez, L., Serrano, L., Rodríguez, A., et al., *Bioresour. Technol.* 100(3): 1262(2008). https://doi.org/10.1016/j.biortech.2008.08.013.
19. Sharma, A.K., Anupam, K., Swaroop, V., et al., *J. Cleaner Prod.* 106: 422(2015). https://doi.org/10.1016/j.jclepro.2014.03.095.
20. Rosli, W.D.W., Law, K.N., Zainuddin, Z., et al., *Bioresour. Technol.* 93(3): 233(2003). https://doi.org/10.1016/j.biortech.2003.11.016.
21. Zhang, T., Guo, M., Cheng, L., et al., *Cellulose* 22(2): 1039(2015). https://doi.org/10.1007/s10570-015-0570-x.
22. Prychid, C.J., Rudall, P.J., and Gregory, M., *Bot. Rev.* 69(4): 377(2003). https://doi.org/10.1663/0006-8101(2004)069[0377:SABOSB]2.0.CO;2.
23. Morais, F.P., Bértolo, R.a.C., Curto, J.M.R., et al., *Mater. Lett.: X* 4: 100028(2019). https://doi.org/10.1016/j.mlblux.2019.100028.
24. Jia, W., Zhou, M., Yang, C., et al., *J. Bioresour. Bioprod.* 7(3): 180(2022). https://doi.org/10.1016/j.jobab.2022.05.002.
25. Yuan, Z., Kapu, N.S., Beatson, R., et al., *Ind. Crops Prod.* 91(30): 66(2016). https://doi.org/10.1016/j.indcrop.2016.06.019.
26. Novo, L.P. and Bras, J., *J. Renewable Mater.* 6(2): 160(2018). https://doi.org/10.7569/JRM.2017.634165.
27. Constant, S., Wienk, H.L.J., Frissen, A.E., et al., *Green Chem.* 18(9): 2651(2016). https://doi.org/10.1039/C5GC03043A.
28. Yuan, J.M., Li, H., Xiao, L.P., et al., *Fuel* 319: 123758(2022). https://doi.org/10.1016/j.fuel.2022.123758.
29. Guan, Y., Shu, T., Gao, H., et al., *Int. J. Biol. Macromol.* 172: 178(2021). https://doi.org/10.1016/j.ijbiomac.2021.01.005.
30. Shakeel, U., Li, X., Wang, B., et al., *Process Biochem.* 117: 198(2022). https://doi.org/10.1016/j.procbio.2022.03.026.

ABOUT THIS PAPER

Cite this article as:
Li, Z., Gao, S., Tang, L., et al., *TAPPI J.* 21(10): 543(2022). https://doi.org/10.32964/TJ21.10.543

DOI: https://doi.org/10.32964/TJ21.10.543

ISSN: 0734-1415

Publisher: TAPPI Press

About this journal